Analysing observed star cluster SEDs with evolutionary synthesis models: Systematic uncertainties

P. Anders[1⋆], N. Bissantz[2], U. Fritze–v. Alvensleben[1], R. de Grijs[3,4]
[1] *Universitäts-Sternwarte, University of Göttingen, Geismarlandstr. 11, 37083 Göttingen, Germany,*
[2] *Institut für Mathematische Stochastik, University of Göttingen, Lotzestr. 13, 37083 Göttingen, Germany*
[3] *Institute of Astronomy, University of Cambridge, Madingley Road, Cambridge, CB3 0HA*
[4] *Department of Physics & Astronomy, University of Sheffield, Hicks Building, Hounsfield Road, Sheffield, S3 7RH*

Accepted —. Received —; in original form —.

ABSTRACT

We discuss the systematic uncertainties inherent to analyses of observed (broad-band) **S**pectral **E**nergy **D**istributions (**SED**s) of star clusters with evolutionary synthesis models. We investigate the effects caused by restricting oneself to a limited number of available passbands, choices of various passband combinations, finite observational errors, non-continuous model input parameter values, and restrictions in parameter space allowed during analysis. Starting from a complete set of *UBVRIJH* passbands (respectively their *Hubble Space Telescope*/WFPC2 equivalents) we investigate to which extent clusters with different combinations of age, metallicity, internal extinction and mass can or cannot be disentangled in the various evolutionary stages throughout their lifetimes and what are the most useful passbands required to resolve the ambiguities. We find the U and B bands to be of the highest significance, while the V band and near-infrared data provide additional constraints. A code is presented that makes use of luminosities of a star cluster system in all of the possibly available passbands, and tries to find ranges of allowed age-metallicity-extinction-mass combinations for individual members of star cluster systems. Numerous tests and examples are presented. We show the importance of good photometric accuracies and of determining the cluster parameters independently without any prior assumptions.

Key words: globular clusters: general – open clusters and associations: general – galaxies: star clusters – galaxies: evolution – methods: data analysis

1 INTRODUCTION

Since the seminal work by Tinsley (1968), evolutionary synthesis has become a powerful tool for the interpretation of integrated spectrophotometric observations of galaxies and galactic subcomponents, such as star clusters. Several groups introduced their evolutionary synthesis codes, e.g., Bruzual & Charlot (1993) [B&C], Leitherer et al. (1999) [STARBURST99], Fioc & Rocca – Volmerange (1997) [PEGASE], Fritze – v. Alvensleben & Gerhard (1994) [GALEV] (all with regular updates), with various input physics (evolutionary tracks vs. isochrones from various groups, different sets of stellar spectral libraries, extinction laws ...). The codes do not only vary in terms of input physics but also regarding computational implementation, interpolation routines etc. A number of publications deals with the intercomparison of various evolutionary synthesis codes (e.g. Worthey 1994, Charlot et al. 1996). The impact of uncertainties in the various model parameters (such as in the descriptions of overshooting and mass loss, stellar spectral libraries etc.) on the resulting colours is challenged by Yi (2003). These publications find a good general agreement among the various models, and assign acceptable uncertainties to the model results. Yi (2003) points out the importance of a proper choice of filters for observing objects characterised by different age ranges. This is justified by the light being dominated by stars in different evolutionary stages at different times. The age-metallicity degeneracy is a major drawback for accurate age determinations, especially for young ages ≤ 200 Myr.

In addition to the choice of the specific evolutionary synthesis model used another important caveat merits discussion here. A common assumption in dealing with evolutionary synthesis is a well-populated stellar initial mass function (**IMF**), up to the model's upper mass limit. While this is probably a justifiable assumption for galaxy-sized systems (although uncertainties regarding the IMF *slope* persist), it certainly breaks down at levels of small (open) star clusters and OB associations, where

⋆ E-mail: panders@uni-sw.gwdg.de

stars are formed purely stochastically (by consumption of the available amount of gas), and these statistics dominate the observed dispersion in cluster luminosities. A great deal of progress has been achieved already on this topic, in particular by Cerviño and collaborators (e.g. Cerviño et al. 2002, Cerviño & Valls-Gabaud 2003). The main conclusion is that for systems more massive than $\approx 10^5 M_\odot$ the impact of the stochasticity of the IMF on the results is – in general – low, and the UV continuum is least affected by stochastic dispersions.

The studies referred to before concentrated on the models themselves. When comparing the model results with observations, in order to constrain the cluster parameters age, metallicity, internal extinction, and mass, one does not only need to take into account the model uncertainties, however. The final parameter uncertainties also depend on the observational errors, the choice of passbands used, their number, spectral coverage and individual filter properties, and the analysis algorithm applied to one's data. The most common way of model-observation comparison for astrophysical purposes is the chi-squared minimisation technique, used e.g. for parameter determination of star clusters (e.g. Maoz et al. 2001, de Grijs et al. 2003a,b), determination of star formation histories of galaxies (e.g. Gavazzi et al. 2002), and photometric redshift determination (e.g. Massarotti et al. 2001). Slightly different, but comparable algorithms, like the least-squares method (e.g. Ma et al. 2002) or maximum-likelihood estimation (e.g. Gil de Paz & Madore 2002, Bik et al. 2003), are used as well. However, see Bissantz & Munk (2001) for a critical discussion about the applicability of chi-squared versus least-squares criteria.

The aim of the present paper is a systematic evaluation of inherent uncertainties in the analysis of observed star cluster spectral energy distributions (SEDs) using evolutionary synthesis models. We define an SED as an ensemble of (absolute) magnitudes in a given set of (broad-band) passbands. We pay special attention to the most appropriate choice of passbands to improve future observation strategies. We will point out severe pitfalls, such as trends caused by finite observational errors and unjustified *a priori* **assumptions.**

2 MODEL DESCRIPTION

In section 2.1 we present the basic properties of our evolutionary synthesis models. Section 2.2 is a *general* **description of our cluster SED analysis algorithm, regardless of whether it is used to study the parameters of observed star clusters or of simulated artificial clusters. In section 2.3 we present the specific properties of the artificial clusters (clusters for which SEDs are taken directly from our models) used to simulate observed clusters and study the performance of our analysis tool. From section 3 onwards only these artificial clusters are used.**

2.1 Input Models

We use the single stellar population (SSP) models presented in Schulz et al. (2002), with important improvements regarding the treatment of gaseous emission in the early stages of the cluster evolution, as presented in Anders & Fritze – v. Alvensleben (2003). These models include isochrones from the Padova group including the TP-AGB phase, and model atmosphere spectra from Lejeune et al. (1997; 1998). These extend from 90 Å through 160 μm for five different metallicities, $Z = 0.0004$, 0.004, 0.008, $0.02 = Z_\odot$ and 0.05 or [Fe/H] = −1.7, −0.7, −0.4, 0 and +0.4 (i.e., matching the metallicities of the Padova isochrones), and gaseous emission (both lines and continuum) due to the ionising flux from young massive stars. The models can be retrieved from http://www.uni-sw.gwdg.de/∼galev/panders/. For a general description of the stellar models see Bertelli et al. (1994) and Girardi et al. (2000), for details about the specific isochrones in our models see Schulz et al. (2002).

All calculations presented here are based on a Salpeter IMF in the mass range of 0.15 to approximately 70 $M_\odot$ (0.15 to approx. 50 $M_\odot$ for super-solar metallicity; following from the Padova isochrones). Stellar synthesis models for a Scalo IMF are presented in Schulz et al. (2002) and Anders & Fritze – v. Alvensleben (2003), and are available from the aforementioned WWW address.

2.2 General description of the analysis algorithm

In order to analyse observed SEDs of star clusters in terms of the individual cluster's age, metallicity, extinction, and mass we calculate a grid of models for a large range of values for each of these parameters **(except mass, which is a simple scaling of the model mass** $[M_{\rm model} = 1.6 \times 10^9 M_\odot]$ **to the absolute observed cluster magnitudes)**. Input parameters for the analysis are the time evolution of the spectra of the SSP models, and the derived magnitude evolution in the various passbands.

The individual uncertainties contributing to the overall photometric uncertainties are: the observational uncertainties, an estimated model uncertainty of 0.1 mag, and an uncertainty of an additional 0.1 mag for passbands bluewards of the B band due to known calibration and model problems in the UV. The total uncertainty is the square-root of the quadratic sum of these individual errors. The observational and model uncertainties are expected to be independent.

Galactic extinction is taken into account by dereddening the observations using the Galactic extinction values from Schlegel et al. (1998).

First, we calculated dust-reddened spectra, using the starburst galaxy extinction law by Calzetti et al. (2000), assuming a foreground screen geometry,

$$k'(\lambda) = 2.659 \times (-1.857 + 1.040/\lambda) + 4.05 \quad \text{for } 0.63\ \mu\text{m} \leq \lambda \leq 2.20\mu\text{m},$$

$$k'(\lambda) = 2.659 \times (-2.156 + 1.509/\lambda - 0.198/\lambda^2 + 0.011/\lambda^3) + 4.05 \quad \text{for } 0.09\ \mu\text{m} \leq \lambda < 0.63\mu\text{m}$$

with a reddened flux

$$F_{\rm red}(\lambda) = F_0(\lambda) \times 10^{0.4 \times {\rm E}_s(B-V) \times k'(\lambda)}$$

and a range of values for the colour excess of the stellar continuum $E_s(B-V)$. Since the gaseous emission is relevant only for a short time and even then not the dominating term, the difference between the colour excess of the stellar continuum and that from nebular gas emission lines (e.g. Calzetti et al. 2000), is neglected.

We emphasise that the Calzetti law is valid only for starburst galaxies, while for "normal" galaxies (i.e., undisturbed and quiescent spiral and elliptical galaxies) it is probably at least marginally incorrect (due to the lower dust content in such galaxies). However, for our systematic uncertainty analysis, the specific shape of the extinction law assumed is of minor importance.

We construct SEDs from these models by folding the spectra with a large number of filter response functions **to obtain absolute magnitudes**. The parameter resolutions are:

- Age: 4 Myr resolution for ages from 4 Myr – 2.36 Gyr, 20 Myr resolution for ages from 2.36 Gyr – 14 Gyr;
- Extinction: the resolution is $\Delta E(B-V) = 0.05$ mag, for $E(B-V) = 0.0 - 1.0$ mag;
- Metallicities: [Fe/H] $= -1.7, -0.7, -0.4, 0$ and $+0.4$, as given by the Padova isochrones;
- **Mass: an arbitrary model mass of $M_{\rm model} = 1.6 \times 10^9 M_\odot$ is used.**

When comparing our observed SEDs with the model SEDs we first determine the mass of the cluster by shifting the model SED onto the observed SED.

A number of these model SEDs (for $M_{\rm cluster} = M_{\rm model}$) are shown in Fig. 1, for the 5 available metallicities and for 5 representative ages used for the artificial clusters considered in this paper (see Section 2.3).

Each of the models in our grid is now assigned a certain probability to be the most appropriate one, given by a likelihood estimator of the form $p \sim \exp(-\chi^2)$, where $\chi^2 = \sum \frac{(m_{\rm obs}-m_{\rm model})^2}{\sigma^2_{\rm obs}}$, where $m_{\rm obs}$ and $m_{\rm model}$ are the observed and the model magnitudes in each band, respectively, and $\sigma_{\rm obs}$ are the observational uncertainties. The summation is over all filters. Clusters with unusually large "best" χ^2 are rejected, since this is an indication of calibration errors, features not included in the models (such as Wolf-Rayet star dominated spectra, objects younger than 4 Myr, etc.) or problems due to the limited resolution of the parameters. The cut-off level is set to a total probability $\leq 10^{-20}$, corresponding to a $\chi^2_{\rm best} \geq 46$. The total probability per cluster is then normalised.

Subsequently, the model with the highest probability is chosen as the "best-fit model". Models with decreasing probabilities are summed up until reaching 68.26 per cent total probability (= 1 σ confidence interval) to estimate the uncertainties in the best-fitting model. These uncertainties are in fact upper limits, since their determination does not take into account effects like the existence of several solution "islands" for one cluster (such as e.g. the age-metallicity degeneracy, see below), and discretisation in parameter space.

For real observations, several passband combinations (containing at least 4 passbands) were used for the analysis, to minimise the impact of calibration errors and statistical effects. A minimum of 4 passbands is required to determine the 4 free parameters age, metallicity, extinction and mass independently (see also Anders et al. 2003, de Grijs et al. 2003a,b).

Only clusters with observational errors ≤ 0.2 mag in all passbands of a particular combination are included to minimise the uncertainties in the results (except for some artificial clusters considered in this paper, for which we adopt errors = 0.3 mag). For each combination, the best-fitting models and their associated parameter uncertainties are determined. For a given cluster all best-fitting models (and the associated uncertainties) originating from the different passband combinations are compared. For each of these best-fitting models the product P of the relative uncertainties

$$\mathrm{P} = \frac{\mathrm{age}^+}{\mathrm{age}^-} \times \frac{\mathrm{mass}^+}{\mathrm{mass}^-} \times \frac{\mathrm{metallicity\ Z}^+}{\mathrm{metallicity\ Z}^-}$$

is calculated (the superscripts indicate the 1σ upper ($^+$) and lower ($^-$) limits, respectively). The relative uncertainty in the extinction is not taken into account, since the lower extinction limit is often zero. The data set with the lowest value of this product is adopted as the most representative set of parameters (with its corresponding parameter uncertainties) for the particular cluster being analysed. In cases where the algorithm converges to a single model, a generic uncertainty of 30 per cent for all parameters is assumed, in linear space, corresponding to an uncertainty of $^{+0.1}_{-0.15}$ dex in logarithmic parameter space. See also Anders et al. (2003) for an application to the star clusters in the dwarf starburst galaxy NGC 1569, and de Grijs et al. (2003a,b) for applications of this algorithm to clusters in the interacting starburst galaxies NGC 3310 and NGC 6745.

2.3 Artificial clusters

In this study we will use artificial clusters to investigate the uncertainties related to our analysis on the basis of a comparison with the model grid. **The SED magnitudes of the "ideal" artificial clusters are taken directly from the models.** Standard parameters of these clusters are: metallicity [Fe/H] $= 0.0 = [\mathrm{Fe/H}]_\odot$, internal extinction $E(B-V) = 0.1$, and ages of 8 Myr ("cluster 1"), 60 Myr ("cluster 2"), 200 Myr ("cluster 3"), 1 Gyr ("cluster 4"), and 10 Gyr ("cluster 5"). In this standard set only a age variations, and neither metallicity nor extinction variations are considered initially, for reasons of clarity. The impact of varying the metallicity and extinction values is treated separately, see especially Sect. 3.3. The cluster mass is the model's mass $1.6 \times 10^9 M_\odot$, the "observational" errors are set to be 0.1 mag in each filter. Unless otherwise indicated, the clusters in this paper will have these standard parameters.

For each of these 5 sets of artificial cluster parameters 10,000 cluster SEDs were generated by adding statistical noise to the magnitudes of the "ideal" cluster. The errors are drawn from a Gaussian distribution with the Gaussian σ corresponding to the "observational" uncertainty (= 0.1 mag as standard value).

All clusters are analysed separately with our algorithm in order to assess under which conditions and to what accuracy their input parameters are recovered by our method. Subsequently, all clusters originating from a given "ideal" cluster are used to calculate median parameters and their as-

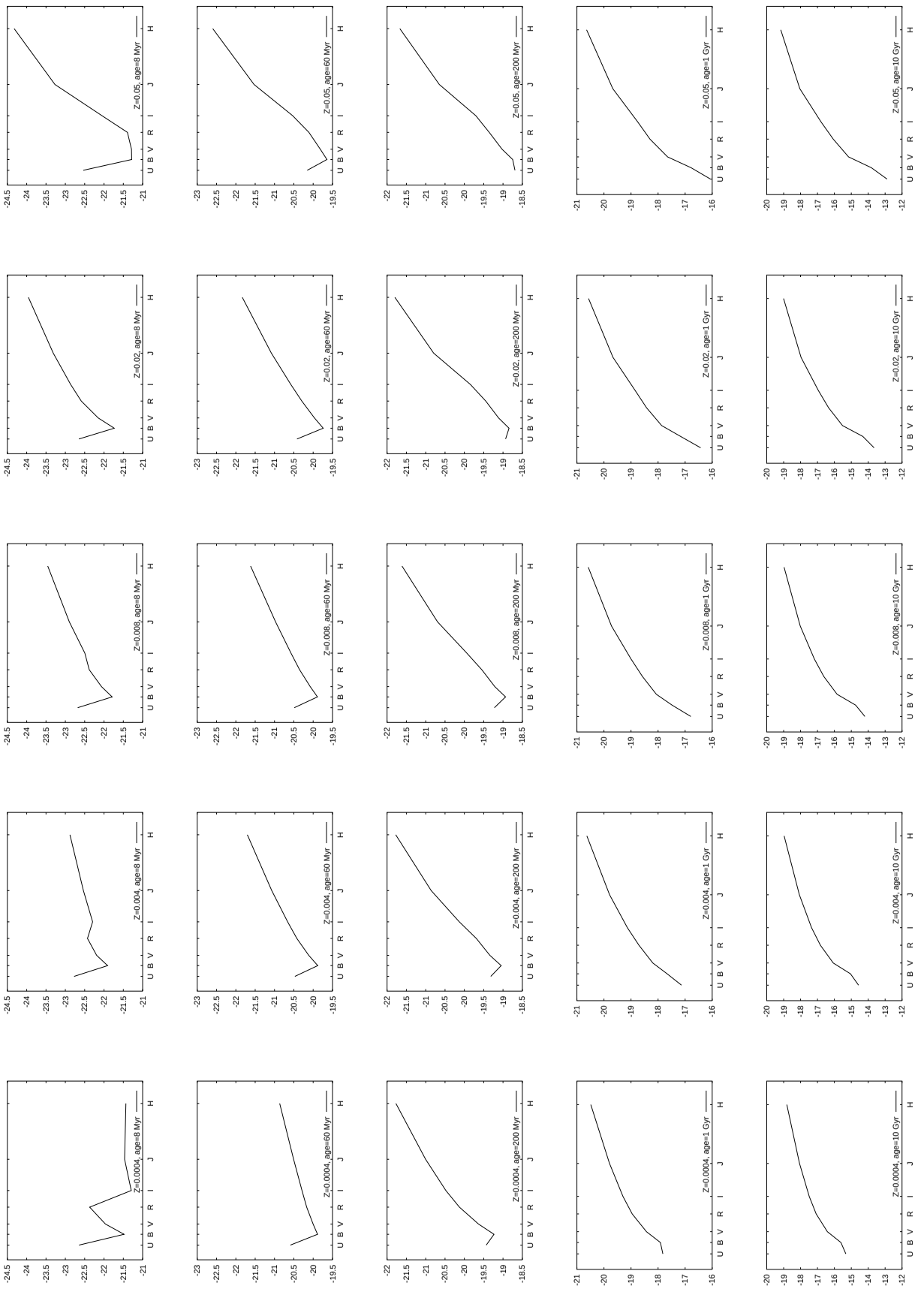

Figure 1. Representative SEDs, for the 5 available metallicities and for 5 different, representative ages. The extinction is set to zero, and a Salpeter IMF is used. **We plot the absolute magnitudes in the respective** *Hubble Space Telescope (HST)* **passbands for** $M_{\rm cluster} = M_{\rm model}$ **as a function of the effective wavelengths of the** *HST* **passbands (see section 3.1); the labels on the horizontal axis are the corresponding standard Johnson passbands.**

sociated uncertainties. The uncertainties are centred around the median solution; they serve as equivalents to the 1σ standard deviation around the average values. However, for our analysis we chose to use the median instead of the average of the distribution, since we believe the median to be physically more relevant. We are interested in finding the most likely result when comparing our model grid with observations.

Free parameters are the metallicity [Fe/H], the extinction $E(B-V)$, log(age) and log(mass). [Fe/H] and log(age) are used instead of Z and age because the evolution of magnitudes is approximately linear in [Fe/H] and log(age).

3 STUDY OF THE ACCURACY OF OUR ANALYSIS

3.1 Passbands included in our analysis

We consider the following filters (the impact of only slightly different filter response curves is small). All filters are taken from the set of available filters for observations of the *Hubble Space Telescope (HST)*/WFPC2, ACS, and NICMOS cameras.

The standard set of filters is: *HST* WFPC2 (and ACS) filters F336W ("*U*"), F439W ("*B*"), F555W ("*V*"), F675W ("*R*"), F814W ("*I*"), NICMOS (NIC2 camera) F110W ("*J*"), F160W ("*H*"). This standard set will be referred to as "*UBVRIJH*". In addition the following filters are included in our study as well: the *HST* WFPC2 (and ACS where appropriate) wide filters F300W ("wide *U*"), F450W ("wide *B*"), F606W ("wide *V*"), F702W ("wide *R*") and the *HST* Strömgren filters F336W ("*u*" ≡ "*U*"), F410M ("*v*"), F467M ("*b*"), F547M ("*y*").

In this paper we will use the term "UV passband" essentially for the U band, and the term "NIR passbands" for the J and H bands.

In the relevant figures, the horizontal lines mark the input values, and the symbols represent the median of the recovered values with the associated uncertainties. The clusters with "cluster number" $= 1 \leq x < 2$ are clusters with the youngest input age of 8 Myr, clusters with "cluster number" $= 2 \leq x < 3$ are clusters with an input age of 60 Myr, and so on (this offset is chosen for reasons of clarity).

3.2 Choice of passband combination

First, we investigate which passbands contain the maximum amount of information, and hence which passbands are preferred for observations, if one can obtain observations in only a limited number of passbands. This aims at improving future observing strategies.

3.2.1 Importance of individual passbands

In Fig. 2 we present the dispersions in our recovered parameters using the standard input parameters, and SEDs covering the full wavelength range *UBVRIJH*, compared with passband combinations where one of the *UBVRIJH* passbands is left out.

This figure provides direct evidence of the importance of the *U* band (and to a lesser degree also of the *B* band) for all stages of cluster evolution, while for ages > 1 Gyr also a lack of the *V* band results in problems to recover the age. The systematic deviations from the input values for the combinations without the *U* or *B* bands are caused by an insufficiently accurate determination of the cluster metallicity. The resulting SED changes are therefore balanced by the analysis algorithm by adjusting the extinction and/or age, and are also accompanied by higher-than-input median masses in our fit results.

Systematic biases are only apparent in the age determination of the oldest artificial cluster (with a slight bias towards younger recovered ages), balanced by an overestimate of the internal extinction (which is a sign of the age-extinction degeneracy) and a minor bias towards smaller median masses. For the 60 Myr-old artificial cluster, the metallicity determination leads to an underestimate (presumably due to the criss-crossing of the models and/or the non-negligible impact of the age-metallicity degeneracy at these ages) for all passband combinations, while for the oldest cluster the uncertainty in the metallicity determination encompasses almost the entire available range.

In general, the median values recovered by our code agree fairly well with the input parameters, with the exceptions mentioned above. The parameter dispersions are largest for the young (ages ≤ 60 Myr) and the oldest (age = 10 Gyr) clusters. This is caused by the criss-crossing of the models for young ages and the flat magnitude evolution for old ages.

The importance of the *U* and *B* band is immediately apparent from the overview of artificial SEDs presented in Fig. 1. *U* and *B* are important for tracing the hook-like structure for young ages, while there appears to be a kink in the SEDs at the *V* band for older ages.

3.2.2 Combinations of 4 passbands

The minimum number of passbands required to determine the 4 free parameters age, metallicity, extinction and mass independently is four.

In Figs. 3 and 4 we present the recovered parameters for *UBVRIJH* compared with various passband combinations consisting of 4 passbands, for optical filters only and including one near-infrared (NIR) band, respectively.

For optical passbands only, the *U* band plays a major role once more, especially in determining the metallicity. Missing *U*-band information leads to underestimates of the metallicity, thereby causing extinction values and ages to be adjusted improperly, and hence this also leads to incorrect mass estimates. Even in cases where the median is recovered correctly, such clusters show the largest uncertainties. In some cases, missing *B*-band information has similar effects, especially for the youngest cluster, while for the oldest cluster the *B* band is vital to break the age-extinction degeneracy. Only for the oldest cluster, the *V* band contains vital information, which is in accordance with our results in Sect. 3.2.1.

For optical+NIR passbands, the situation is similar: The *U* band (and to a lesser degree also the *B* band) is essential. Generally, the offsets from the input values and the uncertainty ranges are smaller than for optical passbands only, thus proving the importance of NIR data. Choosing a NIR band closely resembling the *K* band instead of *J* or *H* would give similar results, possibly restricting the values

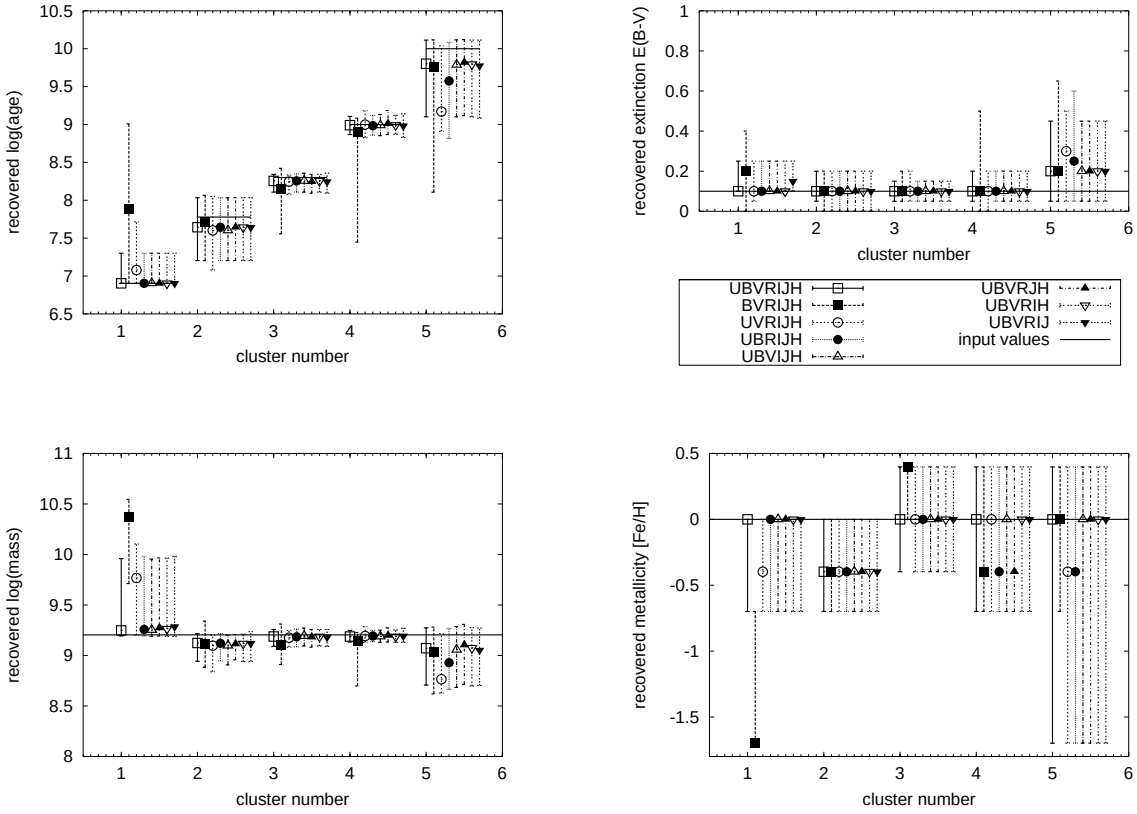

Figure 2. Dispersion of recovered properties of artificial clusters, assuming availability of *UBVRIJH* and passband combinations rejecting one of the *UBVRIJH* passbands, as indicated in the legend. Cluster parameters are standard.

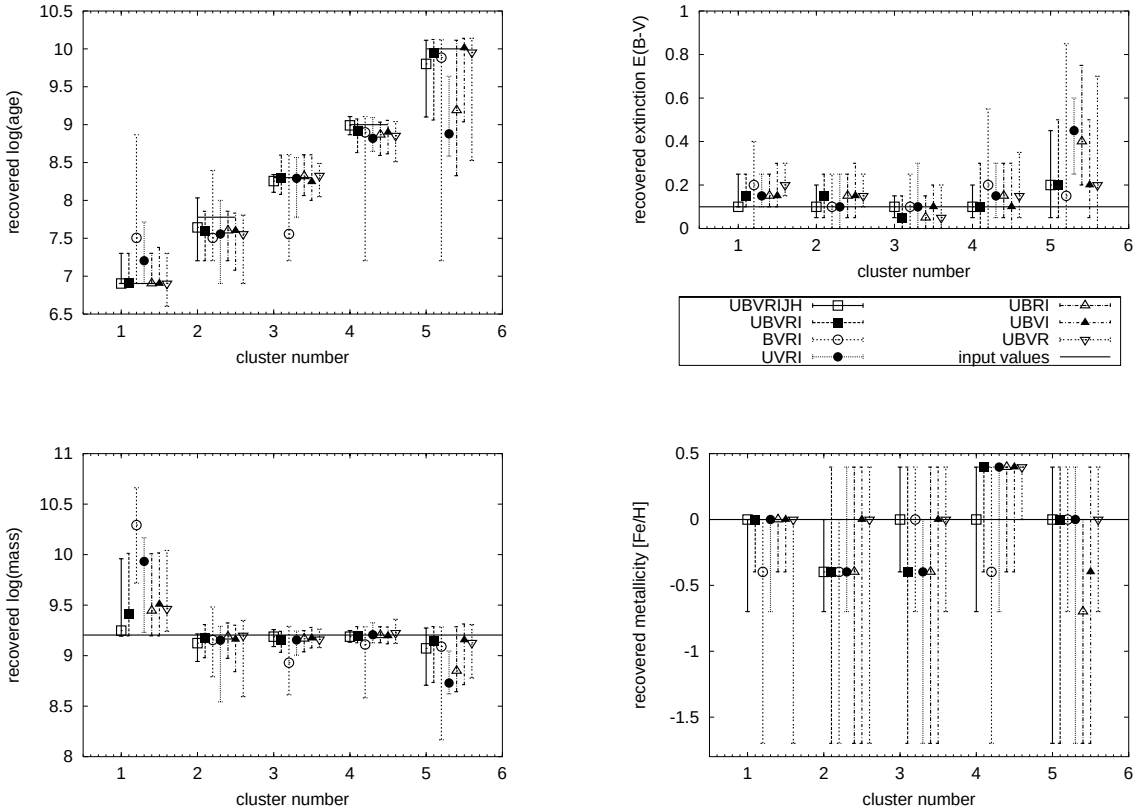

Figure 3. Dispersion of recovered properties of artificial clusters, assuming availability of various optical passband combinations, as indicated in the legend. Cluster parameters are standard.

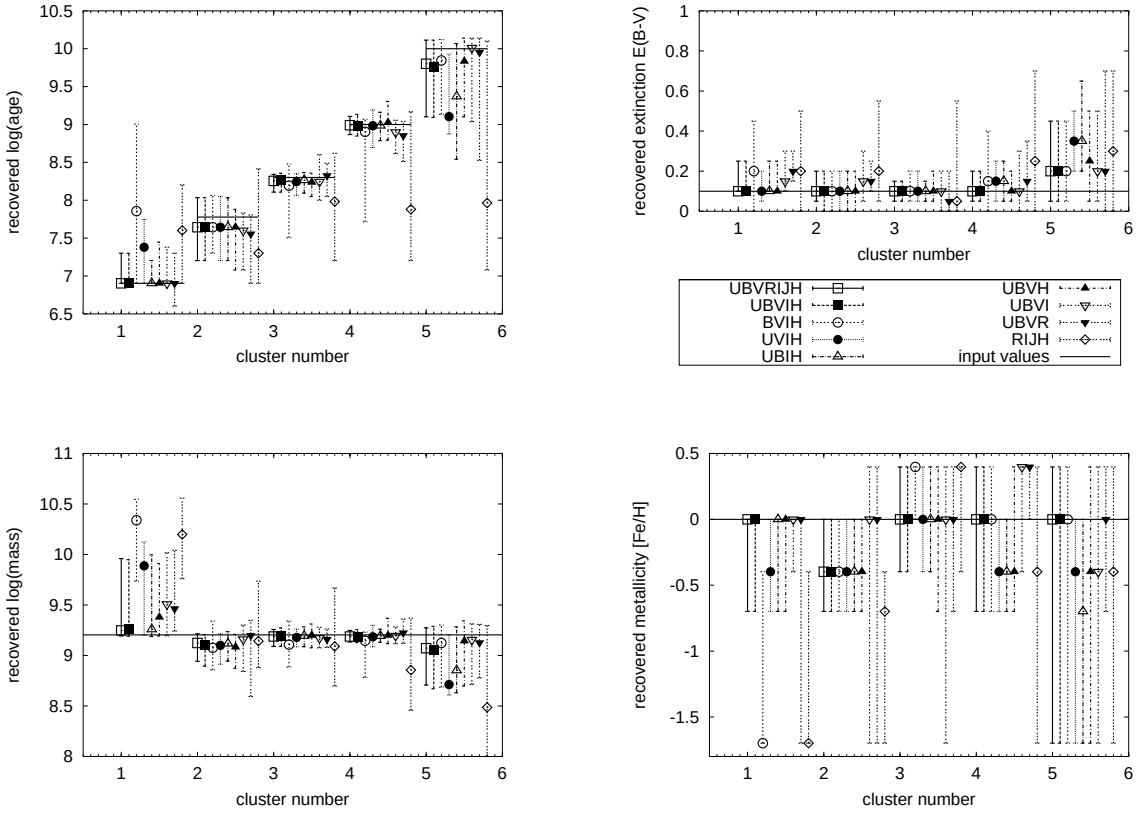

Figure 4. Dispersion of recovered properties of artificial clusters, assuming availability of various optical+NIR passband combinations, as indicated in the legend. Cluster parameters are standard.

slightly better. However, we concentrated on the H band since there are more observations available in H in the *HST* data archive than for filters with longer central wavelengths.

In Fig. 4 we also see the effect of a limited wavelength coverage: in all parameters, the *RIJH* combination gives the worst results (see also de Grijs et al. 2003a). Similar, but less pronounced is the effect for the *UBVR* combination.

Fig. 5 compares the normal WFPC2 *UBVR* system with the corresponding passband combination using the WFPC2 wide filters. In addition, results based on the medium band Strömgren filter system of WFPC2 are shown.

In most cases the wide filter system gives slightly worse results than the standard system. However, driven by the wider filter response curves and the associated smaller observational errors thanks to the larger flux throughput, the wide system might be preferable, e.g., for faint objects.

Using the WFPC2 Strömgren medium-band system does not result in significant improvements compared to wide-band systems. In conjunction with the lower flux throughput (caused by the narrower bandwidth) this system seems less preferable for our purpose. We emphasise that this only holds for our SED analysis.

In de Grijs et al. (2003a) we investigated the impact of the choice of passbands for the young cluster system (with ages of few $\times 10 - 100$ Myr) in NGC 3310 with *HST* data from the UV through to the NIR. Starting with the full set of available passbands, we studied the changes in accuracy of the recovered parameters if we repeated the analysis using only a subset of our passbands. By comparing the results from our analyses using all passbands with those from smaller subsets we found severe biases in the age distributions originating from different passband combinations, in particular for combinations biased towards longer wavelengths (*VIJH*), but also for *UV-UBV* (covering shorter wavelengths only) and *BVIJH*, consistent with the results presented here.

3.2.3 Conclusions on the choice of passbands

From these comparisons we conclude that the passband combinations for the most reliable parameter determination must include the U band, the B band, and use the maximum available wavelength range, preferably including at least one NIR band. If only observations in 4 passbands can be obtained, the best combinations are *UBIH* or *UBVH*, especially for genuinely old objects, and *UBVI*, if NIR data cannot be acquired. We emphasise once again that tracing the kink around the B /V band in the SEDs (see Fig. 1) is vital. For improved metallicity determinations, and consequently for improved determinations of the other parameters as well, NIR data seem to be crucial (for young clusters the U /B bands are also important, in order to determine the metallicity correctly). However, due to the limited metallicity resolution (and the numerous effects the metallicity has on the synthetic magnitudes), the metallicity determination remains the weakest point in our cluster analysis algorithm, and presumably in any routine using synthetic magnitudes from stellar isochrones or tracks.

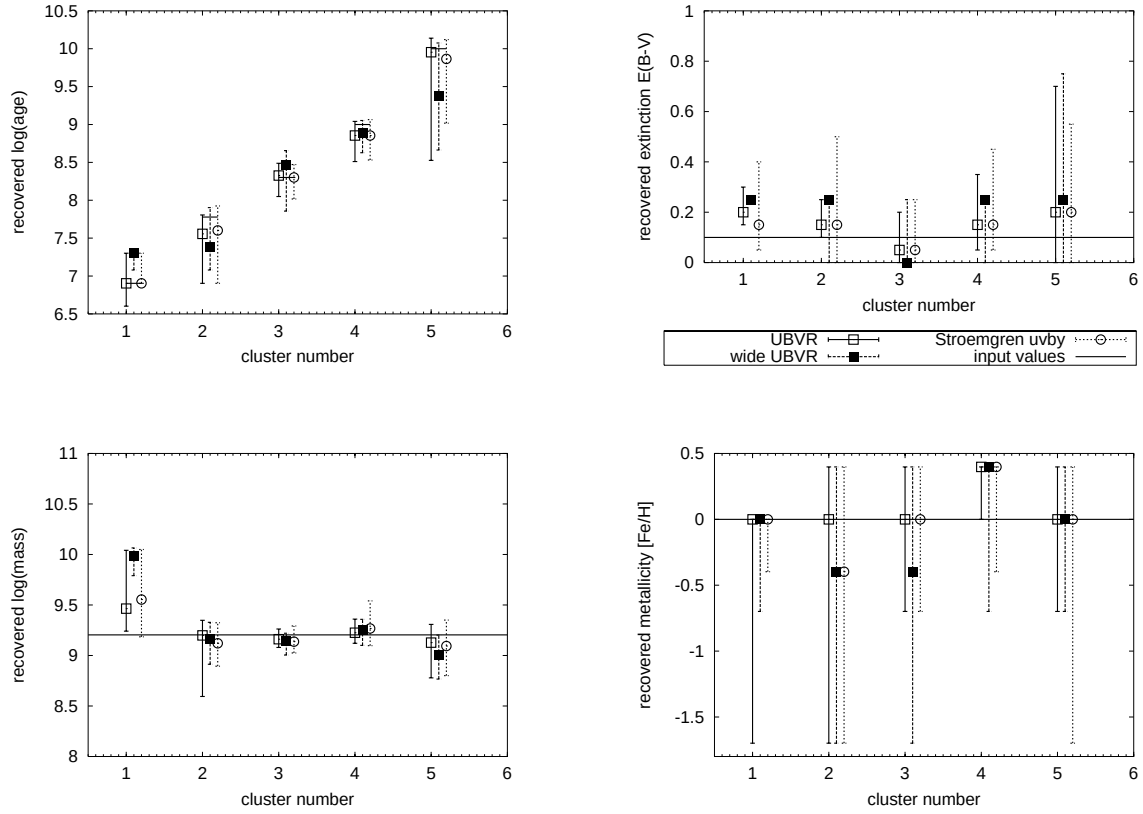

Figure 5. Dispersion of recovered properties of artificial clusters, comparing various wide and medium-band *HST* filters, as indicated in the legend. Cluster parameters are standard.

3.3 Varying the input parameters

In this section we investigate to which extent the input parameters can be recovered as a function of their respective values and observational errors.

3.3.1 Using all 7 filters

Fig. 6 shows, for a range of observational uncertainties, the reliability of our recovered parameters if the standard set of filters (*UBVRIJH*) is available. We caution that we still apply the model uncertainty of 0.1 mag (and an additional uncertainty of 0.1 mag for UV passbands).

A slight trend towards an underestimate of the ages, balanced by a slight overestimate of the internal extinction and an occasional underestimate of the metallicity, is seen. However, even for the largest observational errors of 0.3 mag that we tested for, all recovered parameters are consistent with the input parameters, within the uncertainties.

With increasing observational errors, there seems to be a trend to underestimate the ages for the oldest cluster, balanced by an increasing overestimate of the internal extinction. For genuinely old cluster systems, this degeneracy can be broken by restricting the extinction range. This is generally justified, since such systems are usually dust-poor, if not dust-free, and show fairly homogeneous extinction distributions.

Fig. 7 shows that the degree to which our code recovers the input parameters is largely independent of the input extinction value, with the exception of the ages recovered for the oldest artificial clusters (in this latter case clear signs of the age-extinction degeneracy are apparent). The remaining deviations of the median recovered values from the input values are always less than 0.2 dex, and in most cases even smaller. The deviations in metallicity and extinction are one step in resolution (except for the extinction of the oldest cluster, which is, in most cases, 2 steps off). Small trends for increasing age underestimates with lower input extinction are discernible.

Fig. 8 indicates good agreement between the input parameters and their recovered values for all 5 metallicities. Median extinction values and metallicities match the input values very well. The age determination is correct to Δ log(age) $\lesssim$ 0.25 dex. The mass is recovered very well, as is the extinction. The various metallicity input values are in general correctly recovered, only in few cases a difference of one resolution step is seen.

3.3.2 Using the minimum of 4 filters

The following figures show the accuracy if observations in only the minimum of 4 passbands are available (i.e., a more realistic case). We discuss the best-suited 4-passband-combination identified in Sect. 3.2.2, including the H band, i.e. the combination *UBIH*.

Fig. 9 shows significant trends caused by increasing observational errors, especially for the oldest clusters. For the other clusters, the trends are less severe, with deviations of less than a factor of 2, or one step in the metallicity resolution. For the oldest cluster, the deviations are up to 1 dex in age, 2 steps in metallicity, 0.35 mag in E($B-V$) and 0.5 dex in mass, for the largest observational errors, i.e. 0.3 mag.

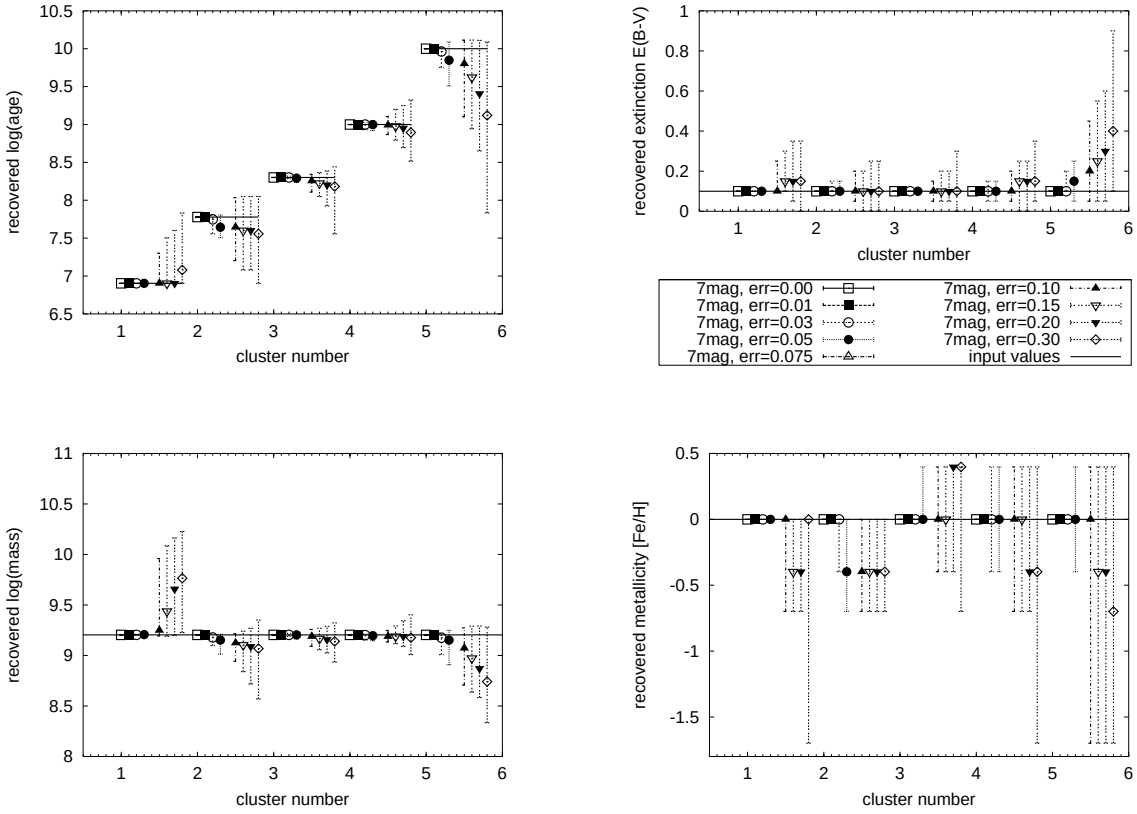

Figure 6. Dispersion of recovered properties of artificial clusters, assuming availability of *UBVRIJH* magnitudes and varying observational errors, as indicated in the legend. Other parameters are standard.

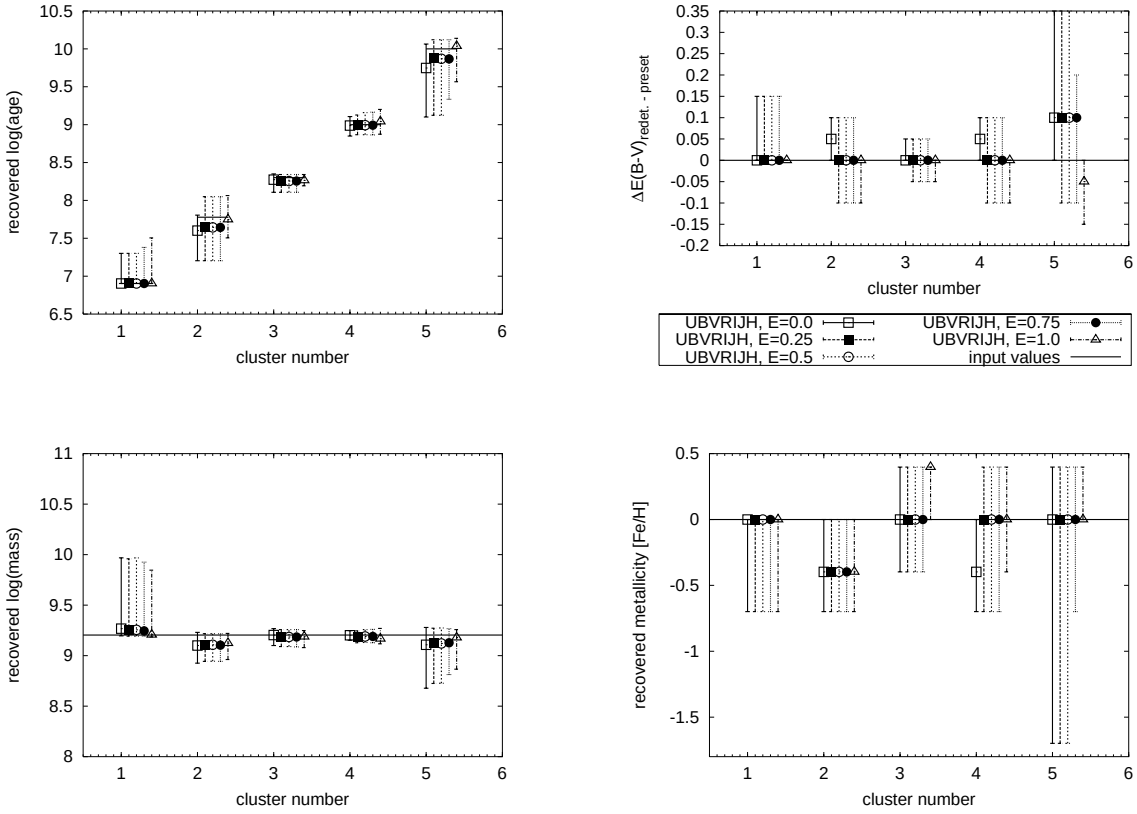

Figure 7. Dispersion of recovered properties of artificial clusters, assuming availability of *UBVRIJH* magnitudes and varying internal extinction values, as indicated in the legend. Other parameters are standard.

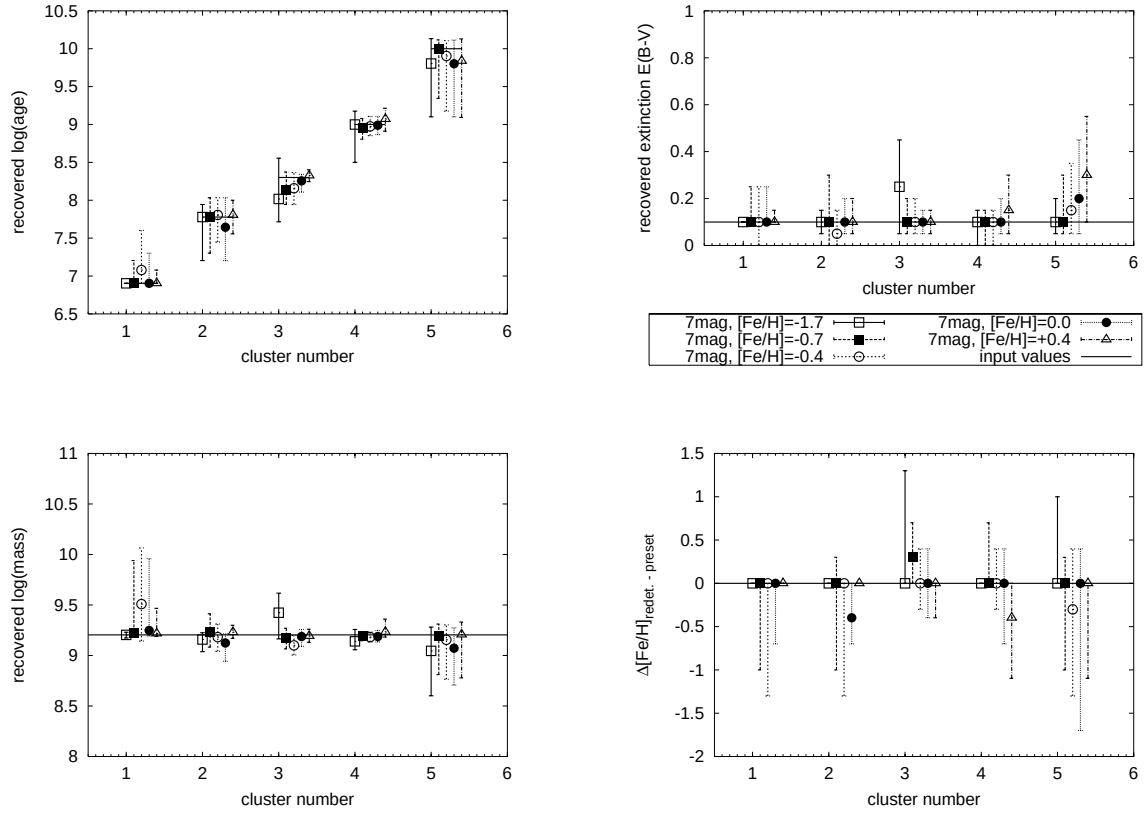

Figure 8. Dispersion of recovered properties of artificial clusters, assuming availability of *UBVRIJH* magnitudes and varying metallicity values, as indicated in the legend. Other parameters are standard.

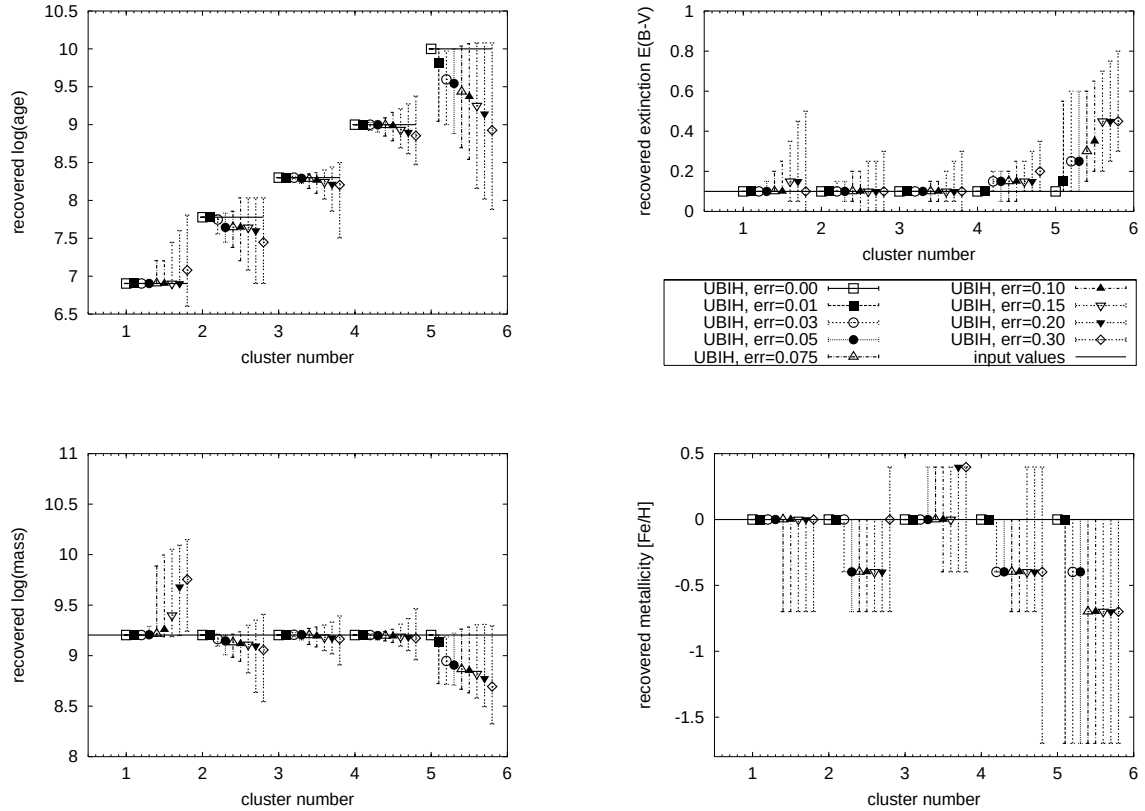

Figure 9. Dispersion of recovered properties of artificial clusters, assuming availability of *UBIH* magnitudes and varying observational errors, as indicated in the legend. Other parameters are standard.

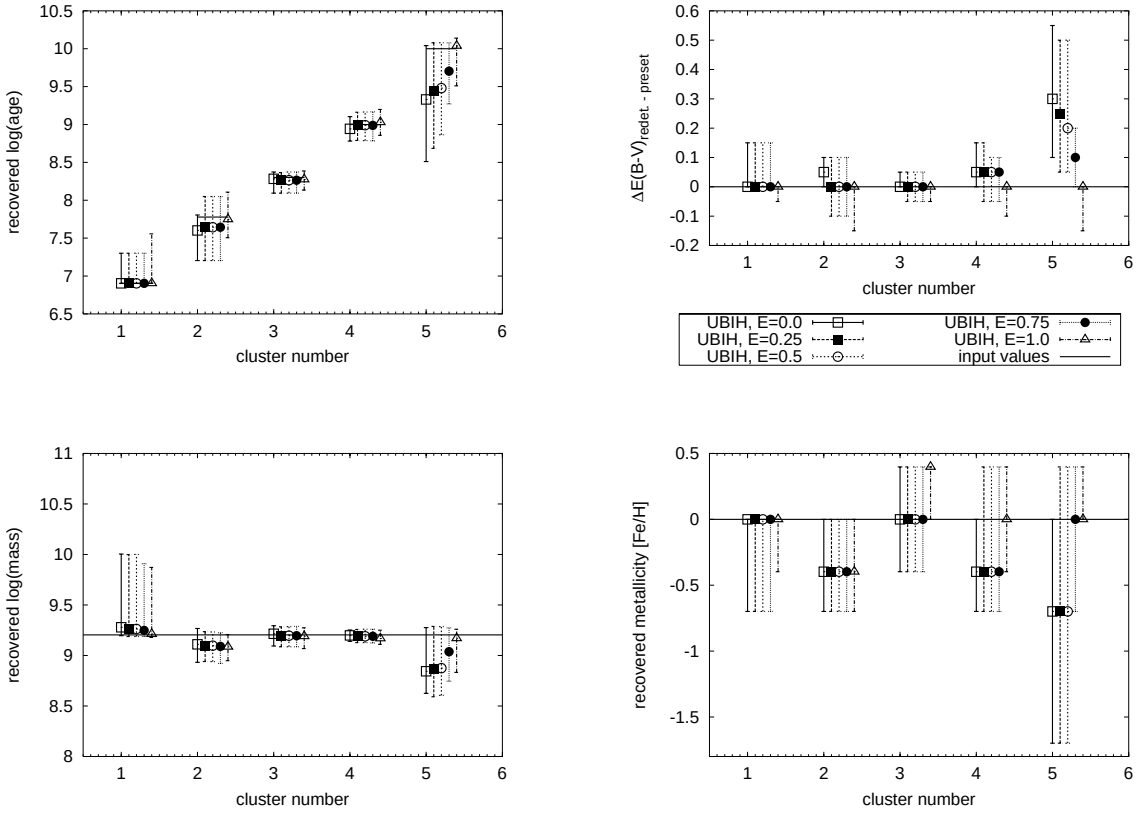

Figure 10. Dispersion of recovered properties of artificial clusters, assuming availability of *UBIH* magnitudes and varying internal extinction values, as indicated in the legend. Other parameters are standard.

Fig. 10 shows the recovered values for *UBIH* and various input extinction values. For all but the oldest cluster, the recovered parameters reproduce the input values very well. The offsets and uncertainties are slightly larger, but comparable to the corresponding values for *UBVRIJH*.

For the oldest cluster there are pronounced trends: with increasing input extinction, the recovered age, metallicity and mass estimates increase, while the offsets of the recovered extinction values from their input values decrease. We find that the higher the input extinction, the better all input parameters are recovered.

Fig. 11 shows the recovered values for *UBIH* and various input metallicities. The trends with increasing input metallicity are less obvious, except again for the oldest cluster (more significant metallicity underestimates and extinction overestimates with increasing input metallicity). This behaviour is also present, but less pronounced for the second oldest (= 1 Gyr old) cluster. For the other, younger clusters, the behaviour appears almost random. This is caused by the slow and steady evolution of magnitudes at large ages: with increasing metallicity the magnitudes become fainter and the colours redder. For younger ages the evolution of the magnitudes is less linear, and they criss-cross several times.

3.3.3 Conclusions on the impact of varying the input parameters

We have investigated the impact of varying the input parameters on the accuracy of our parameter recovery. We find very good agreement, with generally small deviations, by either varying the input extinction or the input metallicity. Only for the oldest artificial clusters there are significant trends in the recovered values with increasing input extinction and metallicity. This can be attributed to a number of degeneracies. **We remind the reader that the upper age limit of the evolutionary synthesis models is 14 Gyr.**

For increasing observational uncertainties there are clear trends of increasing recovered extinction and decreasing ages (with a small increase for the youngest cluster only), mass (an increase for the youngest cluster only) and metallicity. The uncertainties increase as well, as expected.

The results using either *UBVRIJH* or *UBIH* are fairly similar. Using 4 passbands only slightly increases the offsets of the median recovered values from the input values, as well as the uncertainties. Some trends, especially for the oldest cluster, become more significant.

3.4 Restricting the parameter space to the correct ranges

In this section we investigate the consequences of *a priori* restrictions of the parameter space. This might make sense in cases where, e.g., large observational errors may inhibit reasonable parameter constraints or where additional information is available, such as spectroscopic abundances, dynamical age estimates for the starburst event that induced the cluster formation, a low-metallicity dwarf galaxy environment, etc. Here, we explore various cases where we restrict some of our free parameters to the (correct) range of input values, and use passband combinations *UBVRIJH*

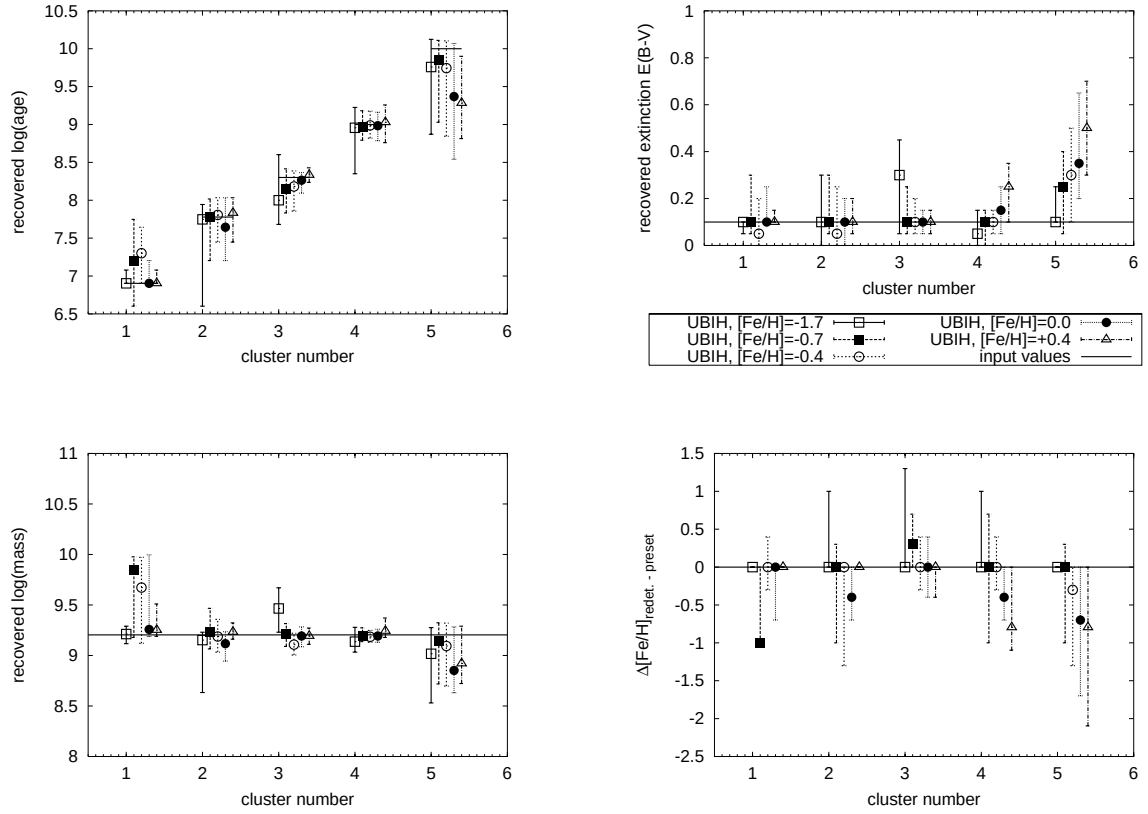

Figure 11. Dispersion of recovered properties of artificial clusters, assuming availability of *UBIH* magnitudes and varying metallicity values, as indicated in the legend. Other parameters are standard.

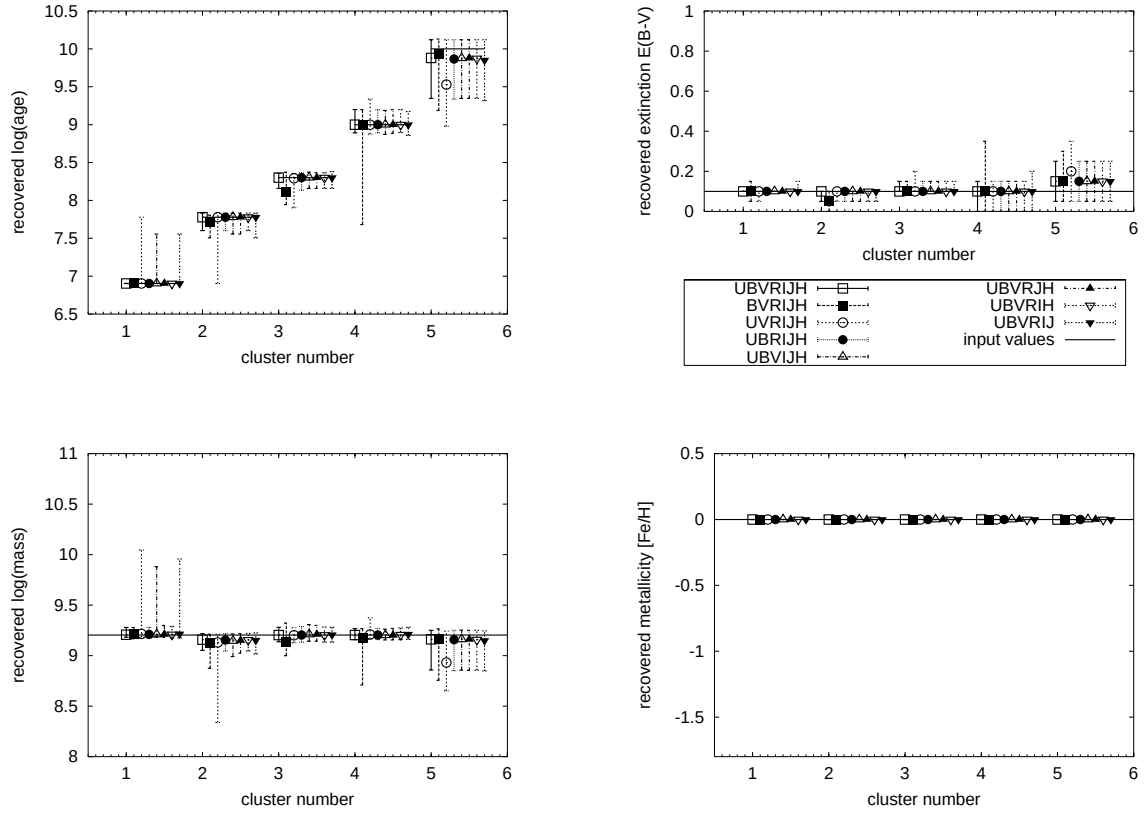

Figure 12. Dispersion of recovered properties of artificial clusters, assuming availability of *UBVRIJH* and passband combinations without one of the *UBVRIJH* passbands, as indicated in the legend. Solutions were sought with metallicity fixed to the input value. Cluster parameters are standard.

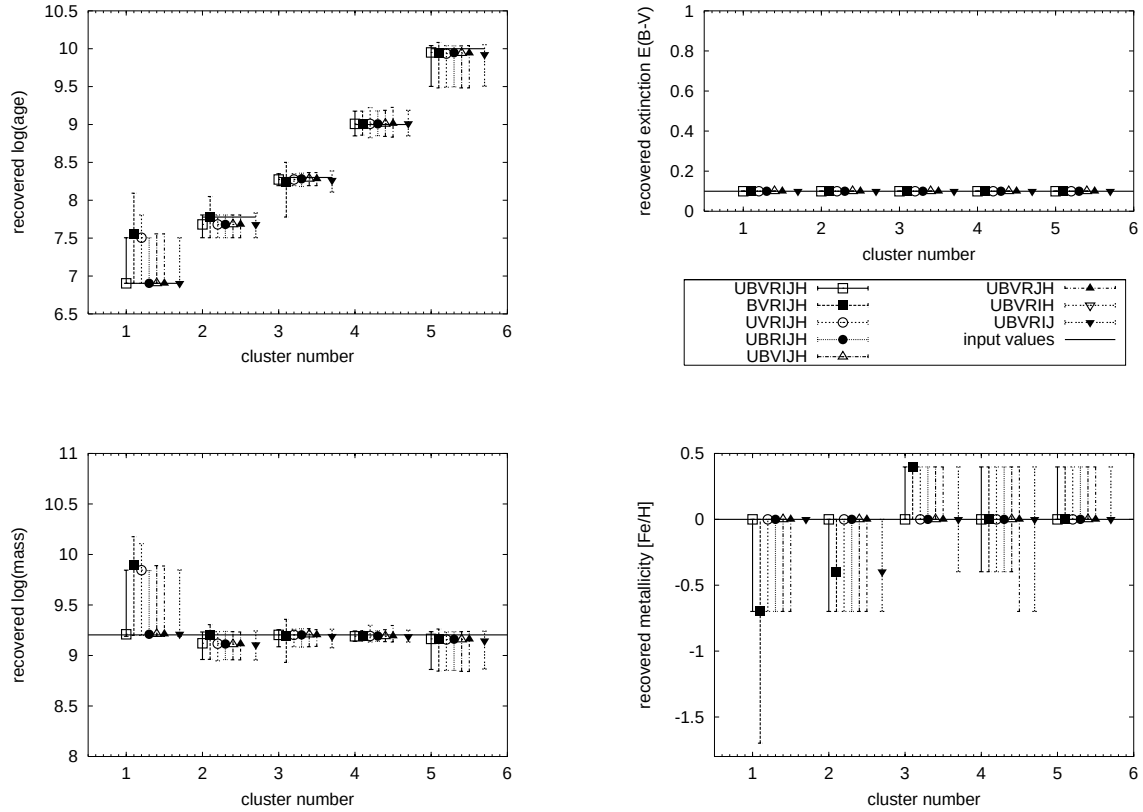

Figure 13. Dispersion of recovered properties of artificial clusters, assuming availability of *UBVRIJH* and passband combinations without one of the *UBVRIJH* passbands, as indicated in the legend. Solutions were sought with extinction fixed to the input value. Cluster parameters are standard.

and combinations lacking one of the *UBVRIJH* passbands to recover the input parameters.

Fig. 12 shows the results when we restrict the metallicity to the (input) solar metallicity. Apart from the oldest cluster (which shows a slight underestimate of the age, balanced by a slight overestimate of the extinction) the recovered values agree almost perfectly with the input values, in any case much better than without metallicity restriction (cf. Fig. 2). The importance of the U and B bands, and of the largest possible wavelength coverage are still reflected by the larger uncertainties for observations lacking those filters. The deviations for the oldest cluster are a result of the age-extinction degeneracy.

In Fig. 13 we investigate the consequences of restricting the analysis to the input extinction, allowing variations only in metallicity and age. The deviations of the median solutions from the input values, and the uncertainty ranges are significantly reduced compared to the unrestricted case shown in Fig. 2. Especially for the oldest cluster, some degeneracies are removed and the recovered values agree much better with the input values than in the unrestricted case. For genuinely old cluster systems the assumption of a generic low extinction may be justified, since such systems are common in old relaxed galaxies with generally low (and uniform) dust content.

Nevertheless, the importance of including the U and B bands is still apparent, especially in the age determination for the youngest cluster. By comparison with Fig. 12 we can attribute this behaviour to the age-metallicity degeneracy.

The results from the restriction of both extinction and metallicity to their input values is presented in Fig. 14. Clearly, all median values agree perfectly with the values of the remaining input parameters. The few large uncertainty ranges indicate passband combinations that still do not allow to determine the solutions unambiguously, because important information (passbands) are missing. Combinations without these passbands do not allow for a reasonable analysis. This includes combinations without the U or B band (and thus insufficient tracing of the kink in the SEDs) and without the U or H band (thereby restricting the wavelength coverage). The R/I bands seem to be of some importance in the early evolutionary stages to trace the curvature of the SEDs.

Restricting the parameter space of our analysis to the input values for some parameters clearly reproduces the input values of the others, and hence can be used as a sanity check for the reliability of the algorithm. We find the age-extinction degeneracy to be most important for old clusters; for such systems a restriction in the allowed extinction range is usually possible. The age-metallicity degeneracy is responsible for some deviations for clusters younger than 200 Myr.

3.5 Restricting the parameter space to incorrect values

In this section we investigate the consequences of *a priori* assuming fixed, but incorrect generic values for the parameters.

First, we investigate the results for various input metallicities, but using solar metallicity to recover the other input

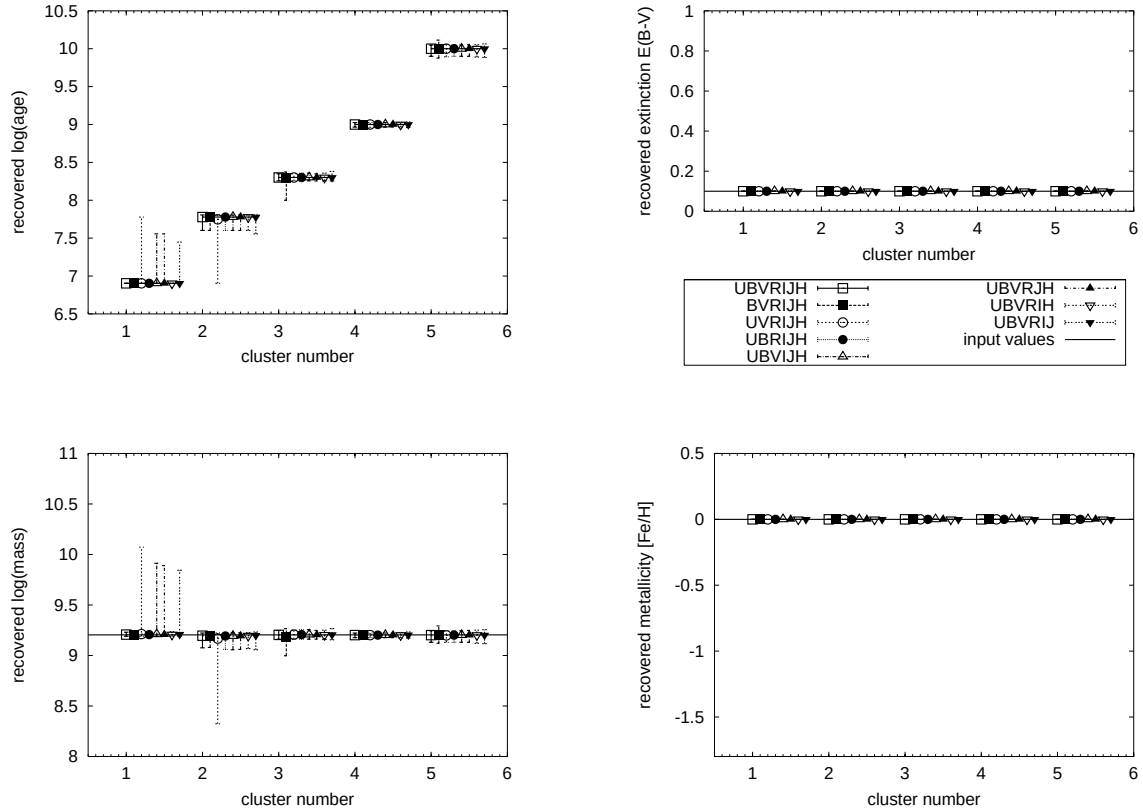

Figure 14. Dispersion of recovered properties of artificial clusters, assuming availability of *UBVRIJH* and passband combinations without one of the *UBVRIJH* passbands, as indicated in the legend. Solutions were sought with extinction and metallicity fixed to the input values. Cluster parameters are standard.

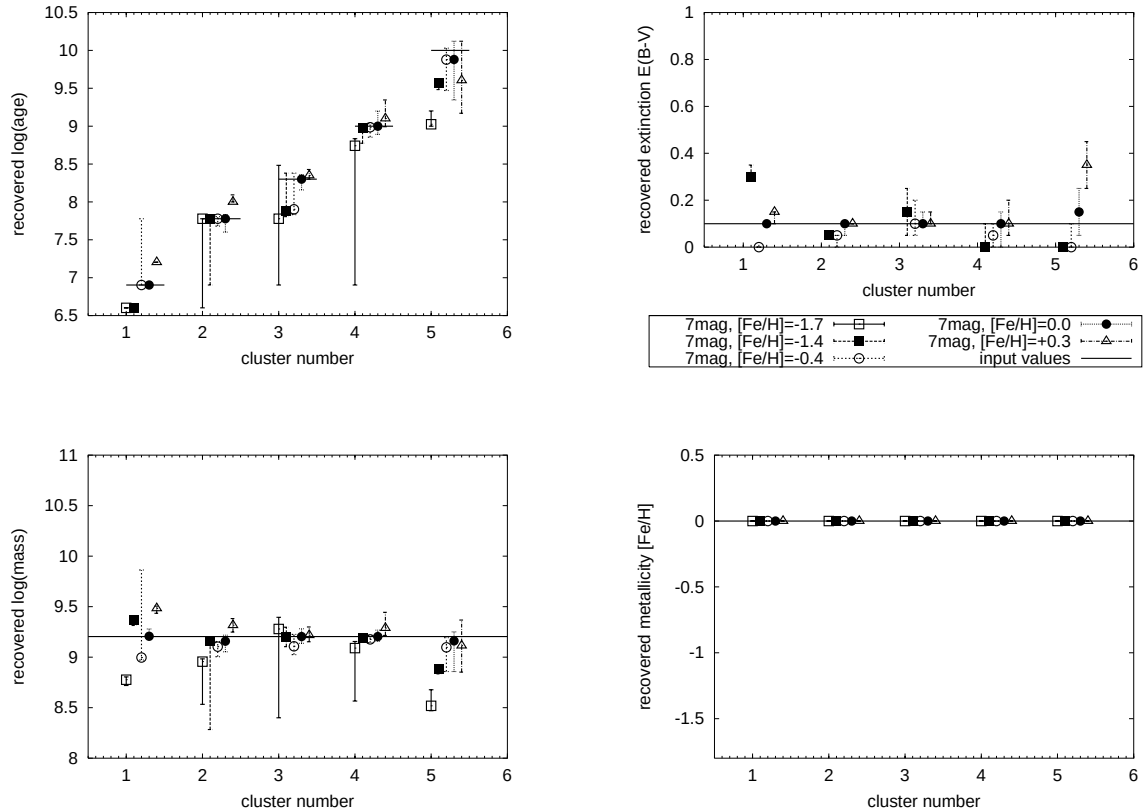

Figure 15. Dispersion of recovered properties of artificial clusters, assuming availability of *UBVRIJH* and various input metallicities, as indicated in the legend. Solutions were sought with metallicity fixed to solar metallicity. Cluster parameters are standard.

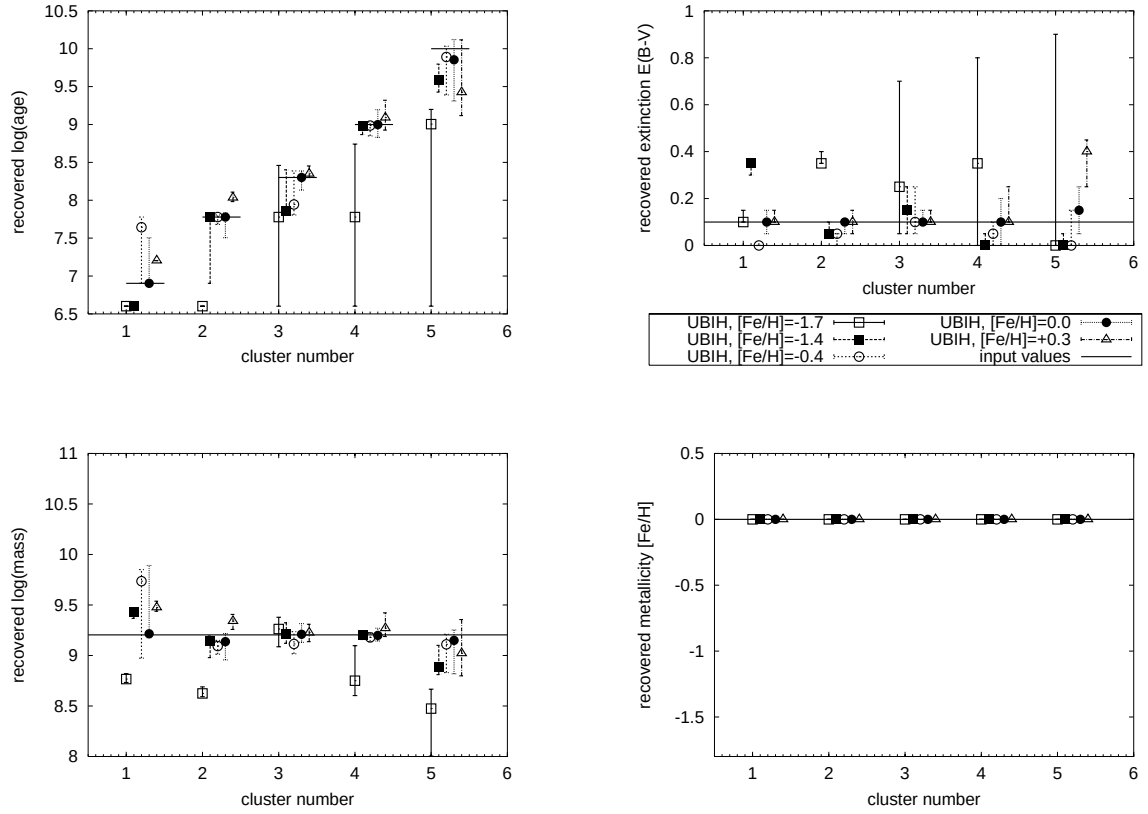

Figure 16. Dispersion of recovered properties of artificial clusters, assuming availability of *UBIH* and various input metallicities, as indicated in the legend. Solutions were sought with metallicity fixed to solar metallicity. Cluster parameters are standard.

parameters (as often done in the literature in studies of interacting and/or merging galaxies). The results are shown in Figs. 15 and 16. There are significant trends in the age determination in the sense of decreasing ages with decreasing input metallicity. These trends are in some cases accompanied by decreasing extinction. If the actual input metallicity is lower than the fixed metallicity assumed for the analysis, the cluster colours will be too blue for the combined input age and extinction, and for the fixed incorrect metallicity. Hence, either the recovered extinction is driven to lower values and/or the solution to younger ages than their respective input values, since both adjustments result in bluer colours for ages $\geq$ 200 Myr. The results for an actual super-solar input metallicity can be understood the other way around. The youngest clusters show rather randomly distributed recovered values, thereby reflecting the complex behaviour of the magnitudes at such young ages. Applying solar metallicity models (as often seen in the literature) for clusters that intrinsically have sub-solar metallicity results in ages that are too low by up to 60 per cent, masses too low by up to 56 per cent and similarly incorrect extinction values if observations in 7 passbands are available, and even more if the observations were obtained in only 4 passbands.

An equivalent test was done for our cluster sample in NGC 3310, where we compared the results from assuming a fixed, solar metallicity to leaving it as a free parameter (see de Grijs et al. 2003a). We found significantly different age distributions in either case, with the analysis in which the metallicity was left as a free parameter resulting in more realistic results in the context of what is known about the starburst in NGC 3310 in general. However, since all clusters are young in this cluster system (with ages of a few $\times 10-100$ Myr), this test was limited to young ages.

In de Grijs et al. (2003b) we concentrated on the impact of restricting the allowed metallicity range for the analysis. By assuming a generic, fixed subsolar metallicity (confirmed by spectroscopy), we found that the derived age distribution is fairly robust compared to the case where the metallicity is left as a free parameter, but the peak of the age distribution is significantly broadened. Hence, there is a larger dispersion for individual clusters. This is presumably caused by clusters that do **not** have the generic metallicity value.

In Figs. 17 and 18 we show the results for *UBVRIJH* and *UBIH*, respectively, if clusters with various extinction values are analysed using a fixed value of $\mathrm{E}(B-V)$. Shown are the results for clusters with input values $\mathrm{E}(B-V) = 0.0, 0.1, 0.25$, and 0.5, but analysed assuming a fixed extinction $\mathrm{E}(B-V)_{\mathrm{fixed}} = 0.1$. Considerable changes are observed in the resulting metallicities and ages. In many cases, the deviations from the input values are much larger than the derived uncertainties. For clusters with ages $\gtrsim$ 200 Myr there are significant trends of increasing recovered ages and metallicities with increasing input extinction. If the actual input extinction is smaller than the extinction fixed for the analysis, the cluster will be too blue for the combination of input age and metallicity, and for the fixed, incorrect extinction. Hence, either the recovered metallicity is driven to lower values and/or the age must be younger than the corresponding input values, since both result in bluer colours. The results for an actual input extinction higher than the fixed value can be understood the other way around. The youngest clusters show less obvious trends in the distributed

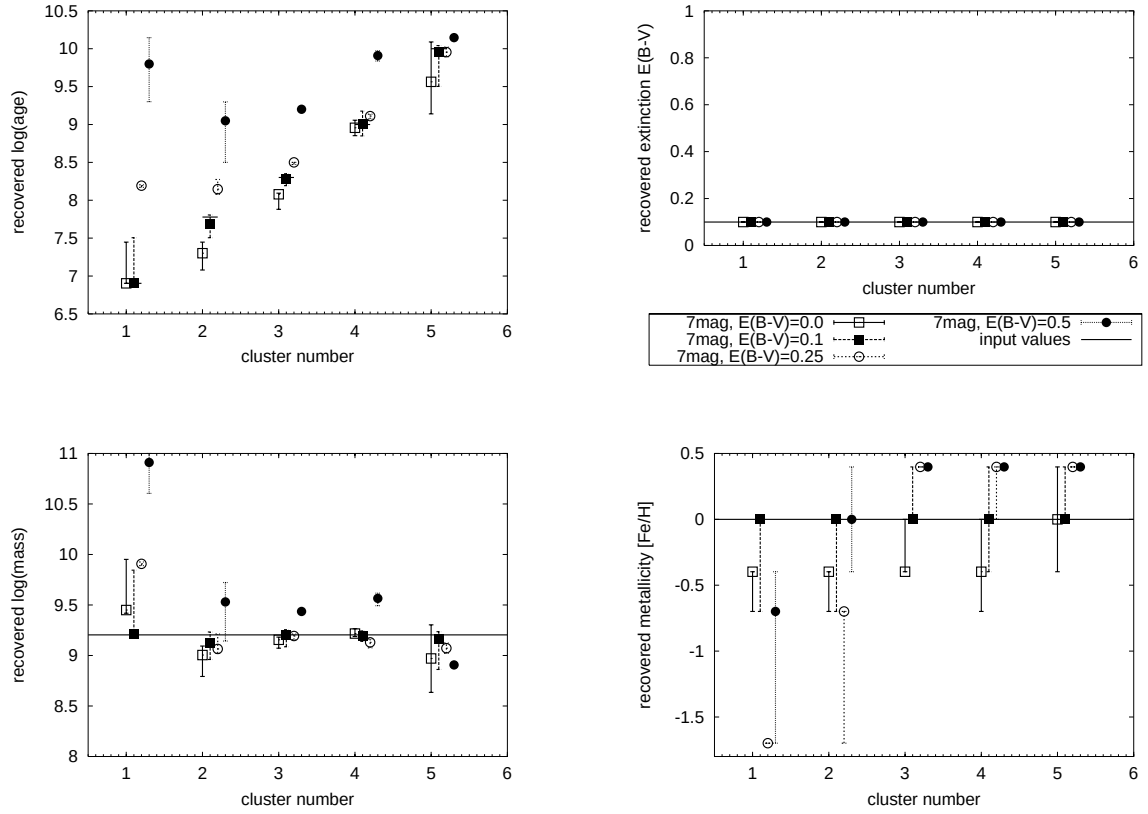

Figure 17. Dispersion of recovered properties of artificial clusters, assuming availability of *UBVRIJH* and various input extinction values, as indicated in the legend. Solutions were sought with extinction fixed to *E(B-V)*=0.1. Cluster parameters are standard.

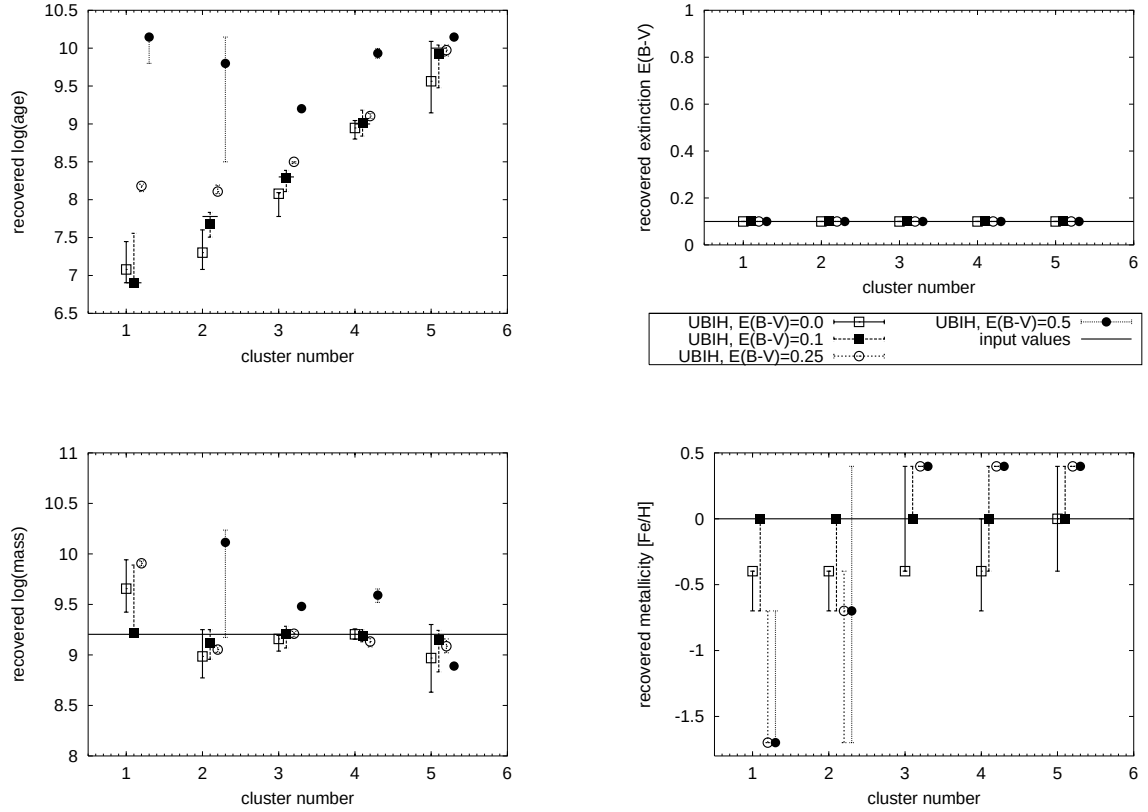

Figure 18. Dispersion of recovered properties of artificial clusters, assuming availability of *UBIH* and various input extinction values, as indicated in the legend. Solutions were sought with extinction fixed to *E(B-V)*=0.1. Cluster parameters are standard.

recovered values with increasing input extinction, showing the complex magnitude behaviour for young ages.

The results from this section again prove the importance of determining the physical parameters of the clusters, such as age, metallicity, and internal extinction (and mass as a derived value), independently, and avoiding any generic assumptions, which might not be justified for all clusters within a given star cluster system. This is true in particular for systems where the existence of two distinct cluster populations is already known or suspected, such as in merging galaxies and galaxies with known colour bimodality in their cluster system.

4 CONCLUSION

We have presented a detailed study of the reliability and limitations of our new algorithm to analyse observed SEDs of star clusters, based on broad-band imaging observations, by comparing these to a grid of model SEDs from our evolutionary synthesis code GALEV.

We have computed a large grid of star cluster SEDs on the basis of our GALEV models for simple stellar populations including all relevant stellar evolutionary phases for ages $\geq$ 4 Myr. The models also include metallicity-dependent gaseous line and continuum emission shown to be an important contributor to broad-band fluxes in early evolutionary stages. Our grid covers ranges in metallicity of $-1.7 \leq$ [Fe/H] $\leq +0.4$, in extinction of $0 \leq \mathrm{E}(B-V) \leq 1$, and ages of 4 Myr $\leq$ age $\leq$ 14 Gyr. The models produce spectra from which we derive absolute magnitudes, and hence broad-band SEDs, for any given filter system. Here, we present results for *HST* broad-band filters widely used for observations and analyses of star cluster systems in external galaxies.

Our parameter analysis algorithm compares a given cluster SED (either observed or theoretical, as done in this study) with the model SEDs from our input parameter grid. Each parameter set is assigned a certain probability, based on an "observation–model" comparison using a chi–squared algorithm. The parameter set with the highest probability is adopted as the best model; the range of parameters from sets with the highest probabilities (up to a total probability of 68.26 per cent) determines the 1σ uncertainties in the parameters.

We constructed numerous artificial cluster SEDs, and varied each of the input parameters in turn to assess their effects on the robustness of our parameter recovery. For each clean model artificial cluster SED we calculated 10,000 additional clusters, with errors distributed around the input magnitudes in a Gaussian fashion.

We identified useful and less suitable passband combinations, with the aim to aid in the planning of observational campaigns. Although a large number of passbands is always preferable, any realistic programme will more likely be limited to observations in the minimum number of required passbands to successfully reach its goals. **In order to successfully disentangle the three free parameters age, metallicity, and internal extinction based on the shape of a broad-band SED, and to determine the mass of a star cluster by simple scaling of the model magnitudes to the observed level, a minimum of four passbands are required.** The most/least preferable passband combinations are summarised in Tables 1 and 2 as a function of the expected age of the cluster population. **In all cases, tracing the kink (or hook) in the SEDs around the B band (see Fig. 1) is of the highest importance. The inclusion of at least one NIR passband significantly improves the results**, since NIR wavelengths allow to efficiently restrict the metallicity range. For the youngest clusters, metallicity estimates are determined by the U and/or B bands. The poorest results are obtained if neither UV information nor B band data are available, or if the available wavelength coverage is very short or biased towards blue or red wavelengths (like *RIJH*).

Table 1. Overview of the most important filters and most/least preferable 4-passband combinations, if NIR data are available

Age	important filters	preferable combinations	combinations to be avoided
$\leq$ few Gyr	*U, B*	*UBIH, UBVH*	*BVIH, RIJH*
$\geq$ few Gyr	*B, V, U*	*BVIH, UBVI*	*UVIH, UBIH*

Table 2. Overview of the most important filters and most/least preferable 4-passband combinations, if no NIR data are available

Age	important filters	preferable combinations	combinations to be avoided
$\leq$ few Gyr	*U, B*	*UBRI, UBVI*	*BVRI, UVRI*
$\geq$ few Gyr	*B, V, U*	*UBVI*	*UVRI, UBRI*

By analysing artificial clusters, using a variety of input parameters (specifically age, metallicity, and internal extinction) with our new code, we find in general good agreement between the recovered and the input parameters. Only the oldest, 10 Gyr-old artificial clusters show significant signs of the well-known age-metallicity-extinction degeneracy.

We have considered several *a priori* restrictions of the parameter space, both to the (correct) input values and to some commonly assumed values. We easily recover all remaining input values correctly if one of them is restricted, *a priori* to its correct input value; this also provides a sanity check for the reliability of our code. We find the age-extinction degeneracy to be most important for old clusters. For such systems, an *a priori* restriction of the allowed extinction range is often possible and shown to be very useful. The age-metallicity degeneracy is responsible for some misinterpretations of clusters younger than 200 Myr.

If we, however, restrict one or more of our input parameters *a priori* to incorrect values (such as using, e.g., only solar metallicity, as often found in the literature), large uncertainties result in the remaining parameters. While certain restrictions might be justified in specific cases, we strongly

advice caution in more complex cases, such as in interacting galaxies or in galaxies with known colour bimodality in their cluster systems.

Finally, we conclude that reliable determination of physical star cluster parameters is possible on the basis of broad-band imaging, provided the availability of a useful set of observational passbands, containing at least four filters, a sufficiently long wavelength base line, and reasonable photometric accuracy. We show that a small, but suitably chosen filter set with deep observations (and the correspondingly small uncertainties) gives more reliable results than a larger number of shallow exposures in inappropriate or redundant filters.

The method we have developed is a versatile and useful tool for the interpretation of large multi-colour data sets for star clusters of different ages and in a large variety of environments, such as provided by, e.g., our ST-ECF/ESO ASTROVIRTEL[1] project "The Evolution and Environmental Dependence of Star Cluster Luminosity Functions" (PI R. de Grijs).

5 ACKNOWLEDGEMENTS

PA is partially supported by DFG grant Fr 916/11-1.

REFERENCES

Anders P., Fritze – v. Alvensleben U., 2003, A&A, 401, 1063
Anders P., de Grijs R., Fritze – v. Alvensleben U., Bissantz N., 2003, MNRAS, submitted
Bertelli G., Bressan A., Chiosi C., Fagotto F., Nasi E., 1994, A&AS, 106, 275
Bik A., Lamers H. J. G. L. M., Bastian N., Panagia N., Romaniello M., 2003, A&A, 397, 473
Bissantz N., Munk A., 2001, A&A, 376, 735
Bruzual G. A., Charlot S., 1993, ApJ 405, 538
Calzetti D., Armus L., Bohlin R. C., Kinney A. L., Koornneef J., Storchi-Bergmann T., 2000, ApJ 533, 682
Cerviño M., Valls-Gabaud D., 2003, MNRAS, 338, 481
Cerviño M., Valls-Gabaud D., Luridiana V., Mas-Hesse J. M., 2002, A&A 381, 51
Cerviño M., Luridiana V., Castander F. J., 2000, A&A, 360L, 5
Charlot S., Longhetti M., 2001, MNRAS 323, 887
Charlot S., Worthey G., Bressan A., 1996, ApJ 457, 625
Fioc M., Rocca – Volmerange B., 1997, A&A 326, 950
Fritze – v. Alvensleben U., Gerhard O. E., 1994, A&A 285, 751
Gavazzi G., Bonfanti C., Sanvito G., Boselli A., Scodeggio M., 2002, ApJ, 576, 135
Gil de Paz A., Madore B. F., 2002, AJ, 123, 1864
Girardi L., Bressan A., Bertelli G., Chiosi C., 2000, A&AS, 141, 371
de Grijs R., Fritze – v. Alvensleben U., Anders P., Gallagher III J. S., Bastian N., Taylor V. A., Windhorst R. A., 2003a, MNRAS, 342, 259
de Grijs R., Anders P., Bastian N., Lynds R., Lamers H.J.G.L.M., O'Neil Jr. E.J., 2003b, MNRAS, 343, 1285
Leitherer C., Schaerer D., Goldader J. D., Delgado R. M. G., Robert C., Kune D. F., de Mello D. F., Devost D., Heckman T. M., 1999, ApJS 123, 3
Lejeune T., Cuisinier F., Buser R., 1997, A&AS 125, 229
Lejeune T., Cuisinier F., Buser R., 1998, A&AS 130, 65
Ma J., Zhou X., Chen J., Wu H., Jiang Z., Xue S., Zhu J., 2002, A&A 385, 404
Maoz D., Barth A. J., Ho L. C., Sternberg A., Filippenko A. V., 2001, AJ 121, 3048
Massarotti M., Iovino A., Buzzoni A., Valls-Gabaud D., 2001, A&A, 380, 425
Moy E., Rocca – Volmerange B., Fioc M., 2001, A&A 365, 347
Schlegel D. J., Finkbeiner D. P., Davis M., 1998, ApJ, 500, 525
Schulz J., Fritze – v. Alvensleben U., Möller C. S., Fricke K. J., 2002, A&A, 392, 1
Tinsley B. M., 1968, ApJ, 151, 547
Worthey G., 1994, ApJS 95, 107
Yi S., 2003, ApJ 582, 202

[1] ASTROVIRTEL is a project funded by the European Commission under 5FP contract HPRI-CT-1999-00081.